GA–A26750

SCALING OF DIVERTOR HEAT FLUX PROFILE WIDTHS IN DIII-D

by

C.J. LASNIER, M.A. MAKOWSKI, J.A. BOEDO, S.L. ALLEN, N.H. BROOKS, D.N. HILL, A.W. LEONARD, J.G. WATKINS, and W.P. WEST

JULY 2010

GENERAL ATOMICS

DISCLAIMER

This report was prepared as an account of work sponsored by an agency of the United States Government. Neither the United States Government nor any agency thereof, nor any of their employees, makes any warranty, express or implied, or assumes any legal liability or responsibility for the accuracy, completeness, or usefulness of any information, apparatus, product, or process disclosed, or represents that its use would not infringe privately owned rights. Reference herein to any specific commercial product, process, or service by trade name, trademark, manufacturer, or otherwise, does not necessarily constitute or imply its endorsement, recommendation, or favoring by the United States Government or any agency thereof. The views and opinions of authors expressed herein do not necessarily state or reflect those of the United States Government or any agency thereof.

GA–A26750

SCALING OF DIVERTOR HEAT FLUX PROFILE WIDTHS IN DIII-D

by

C.J. LASNIER*, M.A. MAKOWSKI*, J.A. BOEDO†, S.L. ALLEN*, N.H. BROOKS, D.N. HILL*, A.W. LEONARD, J.G. WATKINS‡, and W.P. WEST

This is a preprint of a paper to be presented at the Nineteenth International Conference on Plasma Surface Interactions, May 24-28, 2010, in San Diego, California, and to be published in *J. Nucl. Mater.*

*Lawrence Livermore National Laboratory, Livermore, California.
†University of California-San Diego, San Diego, California.
‡Sandia National Laboratories, Albuquerque, New Mexico.

Work supported by
the U.S. Department of Energy
under DE-AC52-07NA27344, DE-FG02-07ER54917,
DE-FC02-04ER54698, and DE-AC04-94AL85000

GENERAL ATOMICS ATOMICS PROJECT 30200
JULY 2010

GENERAL ATOMICS

ABSTRACT

New scalings of the dependence of divertor heat flux peak and profile width, important parameters for the design of future large tokamaks, have been obtained from recent DIII-D experiments. We find the peak heat flux depends linearly on input power, decreases linearly with increasing density, and increases linearly with plasma current. The profile width has a weak dependence on input power, is independent of density up to the onset of detachment, and is inversely proportional to the plasma current. We compare these results with previously published scalings, and present mathematical expressions incorporating these results.

I. INTRODUCTION

The width of the divertor heat flux profile $w_{q,div}$ is of great interest in future large tokamaks as well as many present devices. Previous studies examining the parametric dependence of $w_{q,div}$ have arrived at diverse scalings [1] in JET [2], ASDEX-Upgrade [3], JT60-U [4,5], DIII-D [6,7], and NSTX [8] with results somewhat at variance with each other. We attempt here to perform a new series of experiments in DIII-D to obtain scaling of the divertor heat flux peak value, profile width, and divertor plate power as a function of plasma input parameters, with the maximum number of divertor and scrape-off layer (SOL) diagnostics brought to bear.

We performed measurements in lower single-null edge localized mode (Type I ELMing) H-mode diverted configurations that, due to the strike-point positions, were not strongly pumped (the pump throat was in the private flux region). ELM frequencies ranged from 17 to 97 Hz, except for a point at the lowest plasma current which had an ELM frequency of 325 Hz. We varied the plasma current I_p at constant toroidal field B_T, and varied line-averaged density $\bar{n}_e$ at constant I_p and B_T. The neutral beam injected power P_{inj} was varied at constant I_p and B_T, B_T at constant I_p, and B_T/I_p at constant q_{95}. The divertor heat flux was calculated from infrared camera measurements using a new high-resolution fast-framing IR camera.

The IR camera recorded divertor plate surface thermal emission at 4.8 to 15 kHz frame rates through the whole discharge to allow measuring time-averaged data as well as rapid changes due to ELMs. More than ¾ of the data points were taken a frame rates of 11.4 kHz or greater. Integration times ranged from 32.5 μs to 193 μs. The heat flux at each position in the radial profile was calculated at each of the times steps using the THEODOR 2D heat flux analysis code [9]. We show scaling of the divertor peak heat flux and profile width as a function of the parameters varied, and compare with published results from other devices.

II. PEAK DIVERTOR HEAT FLUX

For each discharge, one or more time intervals of interest were selected where plasma conditions varied little during the interval. The average of each quantity was compiled for each interval. Low-frequency ELMs are included in the average. Including the ELMs increases the resulting peak heat flux by approximately 20%, with a similar increase in the profile width. This procedure was used because it removes an element of judgment in selecting inter-ELM times.

Figure 1 shows the peak heat flux $q_{div,peak}$ at the inner (ISP) and outer strike points (OSP) plotted against the input power P_{in} (neutral beam heating plus Ohmic heating power), where I_p = 1.3 MA, B_T = -1.9 T were held constant. Density was between 5.2 and 6.5×10^{19} m^{-3}, except at the highest power, where $\bar{n}_e = 2.3\times10^{19}$ m^{-3}. Linear fits are shown. A linear dependence of $q_{div,peak}$ on input power can reasonably be concluded, with the caveat that not all points were taken at the same density. Without the highest power point, we still see a linear dependence.

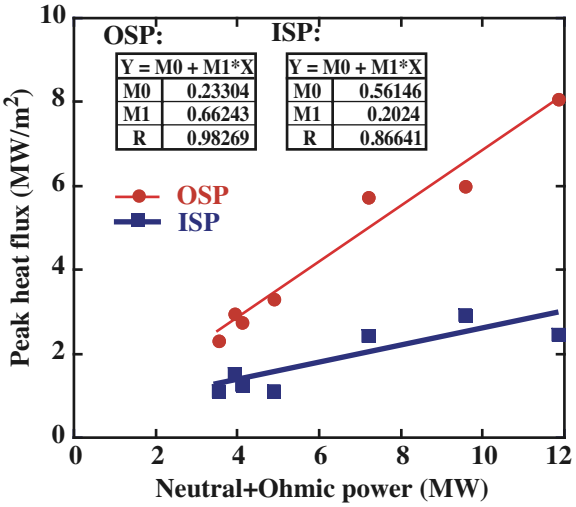

Fig. 1: Peak heat flux at the ISP and OSP plotted against the input power. Linear fits to the data are plotted, with fitting parameters shown in the boxes. The dependence on input power appears to be linear.

Figure 2 again shows $q_{div,peak}$ at the ISP and OSP, this time plotted against line-averaged density, where P_{in} = 4.9-5.1 MW except for the densities $\bar{n}_e = 5.2\times10^{19}$ m^{-3}, where P_{in} = 7.2 MW, and $\bar{n}_e = 6.8\times10^{19}$ m^{-3} where P_{in} = 4.1 MW. Toroidal field was held constant at B_T = -1.9 T, and plasma current was held at I_p = 1.3 MA. Linear fits to the data are shown. If the two density values where P_{in} varied are eliminated, the dependence of $q_{div,peak}$ on density still is linear.

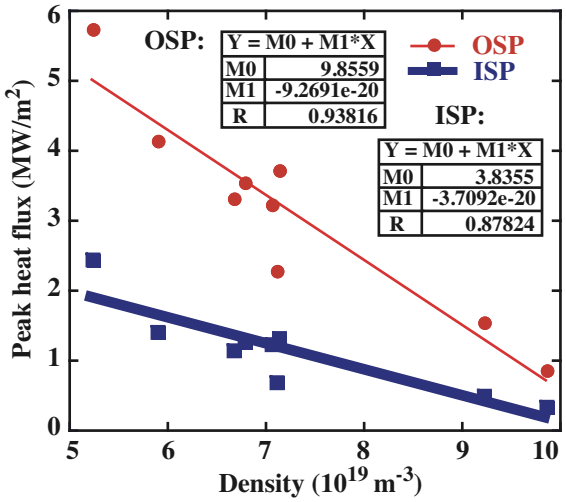

Fig. 2: Peak heat flux at the ISP and OSP plotted against line-averaged density. As density increases, $q_{div,peak}$ decreases linearly.

Figure 3 depicts the $q_{div,peak}$, now plotted against plasma current, showing a linear dependence. Toroidal field was held at B_T =-1.9 T, and P_{inj} = 4.7–5.0 MW except for the point at I_p = 1.3 MA where P_{inj} = 4.1 MW. Density was not held constant, but allowed to vary at the natural H-mode density, because of practical difficulty measuring the heat flux at the OSP during the plasma pumping that would have been required to maintain constant density. Figure 4 shows the line-averaged density variation during the I_p scan. Because of the density variation in this set, this plot does not prove the variation with I_p alone. In combination with the density scan at constant I_p, the dependence on I_p will be extracted from a multi-parameter fit to a larger data set in a later analysis.

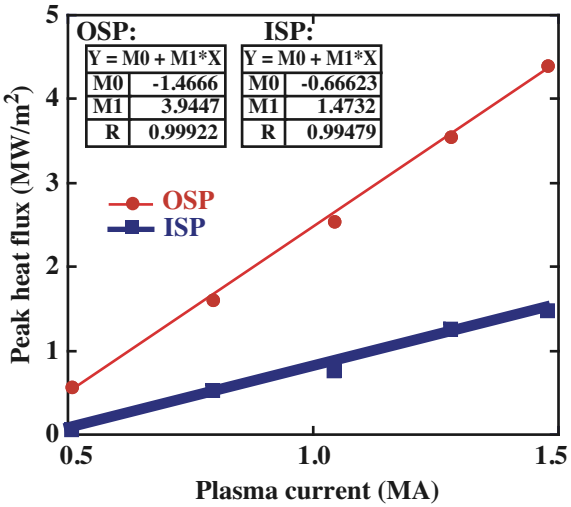

Fig. 3: Peak heat fluxes, now plotted vs I_p. As I_p increases, $q_{div,peak}$ increases linearly.

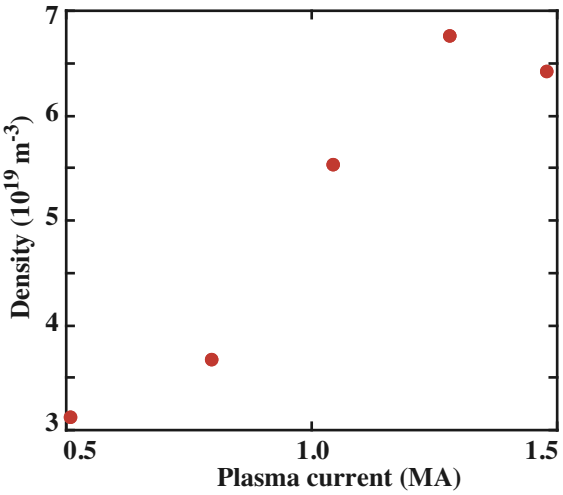

Fig. 4: Line-averaged density variation during the I_p scan. All the densities are below the detachment threshold.

Figure 5 shows $q_{div,peak}$ plotted against B_T at nearly constant safety factor q_{95} = 3.6-3.7, with linear fits. Density ranged from $\bar{n}_e = 3.2 \times 10^{19}$ m^{-3} at the lowest field to $\bar{n}_e = 5.8 \times 10^{19}$ m^{-3} at the highest field. There are not enough data points to conclusively show a linear dependence, but that would be consistent with the data. Since we know from Fig. 2 that the $q_{div,peak}$ decreases with increasing density, this indicates that if density were held constant, $q_{div,peak}$ would increase faster than linearly with increasing toroidal field magnitude at constant q_{95}.

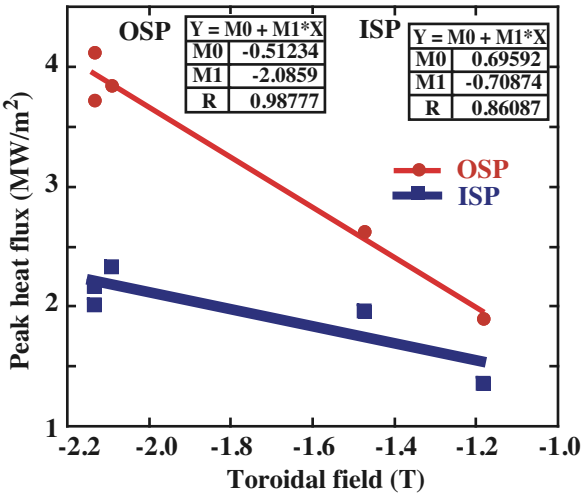

Fig. 5: Peak heat fluxes plotted against B_T at constant q_{95}, showing a reasonable fits to a line. The heat flux variation is primarily due to the change in I_p and not B_T.

The work of Makowski [10] indicates that the heat flux profile width does not depend specifically on the toroidal field. If the width does not change the peak cannot change, by conservation of energy. Therefore most likely the dependence of the peak heat flux

directly on toroidal field is weak if any, and the dependence shown in Fig. 5 is a result primarily of the I_p variation required for maintaining fixed q_{95}. The fits to $q_{div,peak}$ vs input power in Fig. 1 nearly pass through the origin, which we expect it should since there will be no steady-state heat flux at zero input power. We will assume here that the correct fit should pass through zero. We also know from previous work [7] that the heat flux depends as expected on flux expansion from the outer midplane to the divertor plate. This means the dominant dependence of $q_{div,peak}$ at the outer strike point as found above is expressed by

$$q_{div,peak,out} = aP_{in}\left(9.9 - 9.3n_e\right)\left(-1.5 + 3.9I_p\right)\left(R_{div}B_{div}/R_{mp}B_{mp}\right) \quad , \tag{1}$$

where n_e is the line-averaged density in units of 10^{20} m^{-3}, B_{mp}/B_{div} is the ratio of poloidal magnetic fields at the outer midplane separatrix and divertor, and R_{mp} and R_{div} are the major radii at the outer midplane and divertor respectively. The factor $R_{mp}B_{mp}/R_{div}B_{div}$ gives the flux expansion, I_p is in megamperes, and $q_{div,peak,out}$ is in units of MW/m^2. For the inner strike point,

$$q_{div,peak,in} = bP_{in}\left(3.8 - 3.7n_e\right)\left(-0.7 + 1.5I_p\right)\left(R_{div}B_{div}/R_{mp}B_{mp}\right) \quad . \tag{2}$$

For the discharges used here, the flux expansion at the outer strike point was 6.7 and at the inner strike point, 3.1 (again referenced to the outer midplane separatrix). By plotting $q_{div,peak,outer}$ vs the [right hand side of (1)] $/a$ and drawing a line through the data and the origin, we find $a = 0.006 \pm 0.001$ and an analogous procedure for equation (2) gives $b = 0.05 \pm 0.008$. Other fitting parameters in equations (1-4) have a comparable fractional margin of error. The parameters a and b include some geometry dependence such as scaling with size of the tokamak, which is constant within this data set.

III. DIVERTOR HEAT FLUX PROFILE WIDTH

Profile widths discussed here are full width at half maximum (FWHM) values for the ISP and OSP respectively. Widths are obtained at each time point and averaged over the time intervals of interest. Here $w_{q,div}$ shows no dependence on P_{in} (not shown). This is consistent with $q_{div,peak}$ varying linearly with P_{in} in the sense that energy is conserved when P_{in} changes.

Figure 6 shows the outer and inner $w_{q,div}$ plotted against density, for the same density scan as above. There is no effect at low density, but there is a threshold density where the profile becomes wider. Radiated power increases at higher density, but not enough to account for the decreased peak heat flux at the measured widths. It is likely that some energy is deposited in locations that are not measured.

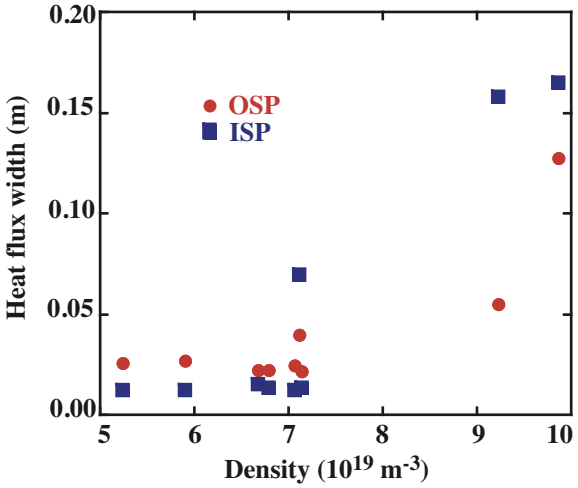

Fig. 6: OSP and ISP heat flux profile widths plotted against density. Density variations below the detachment threshold have no effect on the width.

In Fig. 7 is seen $w_{q,div}$ plotted against I_p, for the current scan already described. We see that widths become larger at low current. The fitted curve for the ISP is linear, but for the OSP, a better fit goes inversely as nearly the first power of the plasma current. No ISP heat flux peak was seen at the lowest I_p. We expect the current dependence of the inner width would be of a similar functional form to that of the OSP if more data were available. In Fig. 3, the peak heat flux for this case at the ISP is very small. The dependence $w_{q,div} \propto 1/I_p$ at least at the OSP from Fig. 7 is consistent with $q_{div,peak} \propto I_p$ from Fig. 3 so that total power is preserved when I_p varies.

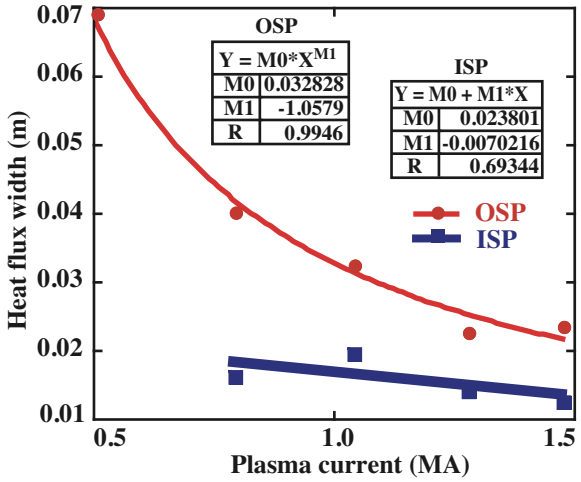

Fig. 7: Profile widths plotted against plasma current. The OSP shows a clear inverse dependence of width on I_p. The inner strike point dependence is less clear, in part because the heat flux is very small at low plasma current.

Because the density scan was performed at constant I_p, we know the effect of density on the heat flux profile width independent of I_p. Fig. 6 shows that the effect of density on $w_{q,div}$ is very weak below the detachment threshold. As shown in Fig. 4, the I_p scan was performed at densities below this threshold so that density dependence does not enter significantly in the I_p dependence depicted in Fig. 7.

The plot in Fig. 8 shows $w_{q,div}$ versus toroidal field at constant q_{95} for the same discharges as described for the peak heat flux scaling. The OSP width decreases linearly with the magnitude of the toroidal field, while the ISP dependence is very weak. This decrease in $w_{q,div}$ is consistent with the increase in $q_{div,peak}$ with increasing magnitude of toroidal field at constant q_{95}.

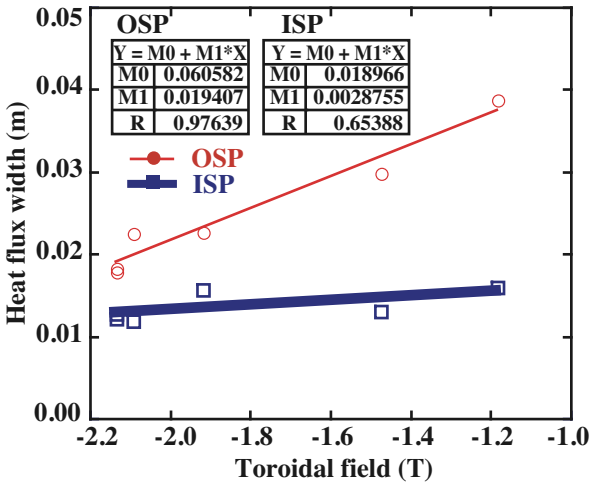

Fig. 8: Profile widths versus toroidal field at constant q_{95}. The trend is described by linear fits. The width variation is primarily due to the change in I_p and not B_T.

As with the discussion of Fig. 5, we know form the work of Makowski [10] that the width does not depend specifically on the toroidal field, and therefore the variation seen in Fig. 8 results primarily from the I_p variation required for maintaining fixed q_{95}. The dependence of the width on power and density are weak (for densities below the detachment threshold). Again taking into account the flux expansion, the dominant $w_{q,div}$ scaling from Fig. 7 for the outer divertor heat flux can be expressed as

$$w_{q,div,out} = 0.0049\left(R_{mp}B_{mp}/R_{mp}B_{div}\right)/I_p^{1.06} \quad , \tag{3}$$

where, I_p is in megamperes, and $w_{q,div,out}$ is in meters. The very small range of variation of inner strike point width in this data set does not yield a useful scaling.

IV. COMPARISONS WITH OTHER EMPIRICAL SCALINGS

Loarte summarized several empirical scalings in Ref. 1, pointing out the areas of disagreement. Here we compare the functional dependences seen above with those scalings.

The linear dependence of $q_{div,peak}$ on power seen above is in agreement with the JET, ASDEX-Upgrade (DIVIII), and previous DIII-D scaling, but not the ASDEX-U (DIVI) scaling. We note that several of those studies use divertor or target power rather than input power. We find the same linear correlation of peak heat flux with target power as with input power.

We have not observed a clear dependence of peak heat flux on toroidal field at fixed I_p in the present data, unlike the previous DIII-D study which found a variation of $1/B_T^{0.5}$. The linear increase in peak heat flux with I_p peak agrees with the previous DIII-D result.

The ASDEX-Upgrade scaling found $q_{div,peak}$ varied inversely with density, which we also see.

The $w_{q,div}$ we use here is different than the λ_q of the referenced studies, which defined an effective width by dividing the strike point power by the peak heat flux. We find in agreement with NSTX, JET and ASDEX-Upgrade (DIVII), essentially no (or very weak) dependence of the width on power. We find in agreement with NSTX that the width decreases with increasing plasma current, approximately as $1/I_p$.

V. CONCLUSION

In the present study we find that peak heat flux varies linearly with input power, inversely as density, linearly with plasma current with a caveat that density was not fixed, and linearly with the magnitude of the toroidal field with q_{95} held constant (primarily because of the change in I_p and not B_T).

We find FWHM $w_{q,div}$ depends not at all on power, and not on density at low density. There is a density threshold for profile broadening associated with the onset of detachment. We see $w_{q,div}$ varies inversely with the I_p and decreases linearly with increasing B_T at constant q_{95}.

REFERENCES

[1] A. Loarte, *et al.*, Nucl Fusion **47**, S203 (2007).

[2] T. Eich, *et al.*, J. Nucl. Mater. **333–339**, 669 (2005).

[3] A. Herrmann, Plasma Phys. Control. Fusion **44**, 883 (2002).

[4] ITER Physics Basis Editors, Nucl. Fusion **39**, 2137 (1999).

[5] A. Loarte, *et al.*, J. Nucl. Mater. **266–269**, 587 (1999).

[6] D.N. Hill, *et al.*, J. Nucl. Mater. **196–198**, 204 (1992).

[7] C.J. Lasnier, *et al.*, Nucl. Fusion **38**, 1225 (1998).

[8] R. Maingi, *et al.*, J. Nucl. Mater. **363–365**, 196 (2007).

[9] A. Herrmann, *et al.*, Plasma Phys. Control. Fusion **37** (1995) 17.

[10] M.A. Makowski, *et al.*, "Comparison of upstream T_e profiles with downstream heat flux profiles and their implications on parallel heat transport in the SOL in DIII-D," these proceedings.

ACKNOWLEDGMENT

This work was supported by the U.S. Department of Energy under DE-AC52-07NA27344, DE-FG02-07ER54917, DE-FC02-04ER54698, and DE-AC04-94AL85000.